sPreparation of biodegradable functionalized polyesters aimed to be used as surgical adhesives

T.M. Cernadas, F.A.M.M. Gonçalves, P. Alves, S.P. Miguel, C. Cabral, I.J. Correia, P. Ferreira

PII: S0014-3057(19)30462-8
DOI: https://doi.org/10.1016/j.eurpolymj.2019.05.019
Reference: EPJ 9040

To appear in: *European Polymer Journal*

Received Date: 6 March 2019
Revised Date: 2 May 2019
Accepted Date: 11 May 2019

Please cite this article as: Cernadas, T.M., Gonçalves, F.A.M.M., Alves, P., Miguel, S.P., Cabral, C., Correia, I.J., Ferreira, P., sPreparation of biodegradable functionalized polyesters aimed to be used as surgical adhesives, *European Polymer Journal* (2019), doi: https://doi.org/10.1016/j.eurpolymj.2019.05.019

Preparation of biodegradable functionalized polyesters aimed to be used as surgical adhesives

T. M. Cernadas[a], F. A. M. M. Gonçalves[a], P. Alves [a], S. P. Miguel[b], C. Cabral[b], I. J. Correia[a,b], P. Ferreira[a,*]

[a] CIEPQPF, Department of Chemical Engineering, University of Coimbra, P-3030 790 Coimbra, Portugal

[b] CICS-UBI, Health Sciences Research Center, University of Beira Interior, P-6200 506 Covilhã, Portugal

[*]Corresponding author: P. Ferreira, CIEPQPF, Department of Chemical Engineering, University of Coimbra, P-3030 790 Coimbra, Portugal

E-mail address: pferreira@eq.uc.pt

ABSTRACT

The study and development of new biocompatible materials to be applied as UV-curable adhesives is extremely important to grant the preparation of matrices with suitable mechanical, biological and thermal properties with a fast curing rate. Herein, photocrosslinkable biodegradable copolymers composed of unsaturated polyesters (UP) and lactic acid oligomers functionalized with 2-isocyanatoethyl methacrylate (IEMA) were produced. Henceforth, three different stoichiometric proportions were tested, which, after the addition of a biocompatible photoinitiator (Irgacure® 2959), resulted in flexible, resistant and uniform matrices after 2 minutes and 30 seconds of crosslinking.

The synthesized materials were then further characterized in terms of chemical composition and thermal/mechanical behaviour. The gel content, dynamic contact angles, water sorption capacity and hydrolytic degradation were also assessed. The biocompatibility and antibacterial activity of the produced materials was also evaluated.

Taking into account all the data obtained, it may be concluded that the new synthesized biodegradable bioadhesives present promising properties to be used as surgical adhesives.

Keywords: Surgical adhesive; polyester; photocrosslinkable copolymers; biocompatibility; biodegradability.

1. Introduction

Surgical adhesives emerge as an alternative to traditional methods used in the treatment and regeneration of biological tissues. They must be able to hold both wound edges together until the tissues present sufficient mechanical strength to properly withstand wound healing. These devices, must be able to polymerize in a moist environment and biocompatible products should be formed as result of their degradation [1,2]. The development of these materials promotes the enhancement of surgical practices, leading to an improvement of the patient's quality of life. Amongst the main characteristics that make the surgical adhesives so attractive, the reduction of induced trauma in the surrounding tissues, the speed and ease of application, their biodegradation and the unnecessary post-surgical removal may be highlighted [1–3].

Currently there are several types of commercially available surgical adhesives classified as natural or biological (e.g. fibrin glues [4], collagen adhesives [5,6]), synthetic and semi-synthetic (gelatin-resorcinol-formaldehyde [7], cyanoacrylates [8]) and biomimetics (marine mussel extracts [9]). However, the use of blood derived products such as fibrin has been associated with the risk of diseases transmission, while cyanoacrylates degrade into formaldehyde, which confines their use to external applications [1,10,11]. One possible solution to circumvent these limitations is the development of adhesives based on biodegradable and biocompatible polymers. Among them, the use of photocrosslinkable polymers has been regarded as an appealing strategy, since they can be produced *in situ*, *i.e.*, the exposition of the polymers to an irradiation source (usually UV) will resulted in stable polymeric matrix, in a short period. Further, it is possible to tailor the properties of the adhesives (e.g. mechanical strength, hydrophilicity, porosity) through the control of some parameters, such as polymer formulation, type and amount of photoinitiator, beam wavelength and irradiation time [12–16].

The photopolymerization and photocrosslinkage of polymers aimed for the preparation of surgical adhesives has been widely developed over the years. More specifically, synthetic aliphatic polyesters and its copolymers have arisen interest, mainly due to their ester linkage susceptibility to hydrolytic and enzymatic degradation under physiological conditions. Also, the products resulting from that degradation are

naturally occurring metabolites [3]. Among synthetic aliphatic polyesters, the most broadly used in the biomedical field is poly(lactic acid) (PLA) [17], a polymer approved by the Food and Drug Administration (FDA). It has been widely used for the production of biodegradable sutures, clamps, scaffolds and drug delivery systems [16,18–20]. Some authors have already reported the functionalization of PLA with photocrosslinkable groups intended for surgical application [16,21–25]. These materials have shown good adhesion results and a fast-curing rate at physiological temperature. Nevertheless, its application as a tissue adhesive has not been extensively studied, due to the low solubility in non-toxic solvents, high molecular weight and glass transition of the commercial PLA. Furthermore, the biodegradation rate is still an issue when it comes to the use of PLA as a surgical adhesive for internal application. Therefore, the copolymerization of PLA with other polymers with higher degradation rates is a common strategy. Thus, the use of unsaturated polyesters (UP) can allow the enhancement of the copolymer properties including hydrophilicity, biodegradation rate, biocompatibility and bioadhesion of the synthesized materials [26].

The present work aimed to accomplish the synthesis of copolymers, based on lactic acid oligomers (OligLA) and an UP prepared from polyethylene glycol (PEG) and fumaric acid by bulk polycondensation. The incorporation of this UP in the copolymers final structure aimed to improve the hydrophilicity and biodegradation rate of the materials. In order to further crosslink the prepared polymers, OligLA was functionalized with 2-isocyanatoethyl methacrylate (IEMA), an isocyanate-functional monomer containing carbon double bonds. Henceforth, three different stoichiometric proportions were tested using a biocompatible photoinitiator Irgacure® 2959 (Ir2959) [27]. Finally, the viability of the materials for the intended application was evaluated through the characterization of their chemical and thermal properties. Their biological performance was also assessed by studying their interaction with cells and bacteria.

2. Experimental Procedures

2.1. Materials

Fumaric acid (FA, 99%), poly ethylene glycol (Mn≈600), hydroquinone, potassium hydroxide (85%), ethanol (96%), phenolphthalein, aqueous solution of L(+)-lactic acid

(LA, 80%) and deuterated tetrahydrofuran (THF, 99.5%) were purchased from Sigma-Aldrich (Sintra, Portugal).

The functional monomer 2-isocyanatoethyl methacrylate (IEMA, 98%) was acquired from TCI (Belgium). The photoinitiator 2-hydroxy-1-[4-(2-hydroxyethoxy) phenyl]-2-methyl-1-propanone, trade name Irgacure® 2959 (Ir2959), was provided by Ciba Specialty chemicals. All reagents were used as received without further purification. The co-monomer 1,4-butanediol (99%) and diethyl ether (99%), used as solvent were purchased from ACROS Organics.

Fetal bovine serum (FBS) (free from any antibiotic) was obtained from Biochrom AG (Berlin, Germany). Normal Human Dermal Fibroblasts (NHDF) cells were acquired from PromoCell (Labclinics, S.A., Barcelona, Spain). 3-(4,5-Dimethylthiazol-2-yl)-2,5-diphenyltetrazolium bromide (MTT) was bought from Alfa Aesar (Ward Hill, USA). Amphotericin B, Dulbecco's modified Eagle's medium (DMEM-F12), Phosphate-buffered saline solution (PBS), PCL (80,000 Da), Trypsin were attained from Sigma-Aldrich (Sintra, Portugal). *Staphylococcus aureus* clinical isolate (S. aureus) ATCC 25923 and *Escherichia Coli DH5 α* (E. coli) were used as model organisms to evaluate the bactericidal activity of the bioadhesive.

2.2. Synthesis procedures

2.2.1. Synthesis of the unsaturated polyester

The UP was prepared by bulk polycondensation, in the molar ratio of 1:1. FA, the source of double bonds, PEG 600 and the inhibitor, hydroquinone (0.02% of the total weight) were charged into a three-neck round-bottom glass flask, equipped with a nitrogen inlet with constant flow, a glass condenser and magnetic stirring. The reactor was first heated at 160 °C, and then the temperature was raised to a maximum of 220 °C along the reaction. The polycondensation was carried out for at least 15 h. The end of the reaction was determined by monitoring the acid value (AV), according to ASTM 109-01.

2.2.2. Synthesis of the lactic acid oligomers and further functionalization

OligLA with two OH end groups (linear structure) was synthesized by conventional polycondensation, under atmospheric pressure, using 1,4-butanediol as a co-monomer. The oligomer was synthesized by reacting lactic acid with 1,4-butanodiol, in the molar ratio of 6:1, in a heated three-neck round-bottom glass flask, equipped with a magnetic stirrer, a glass condenser and under nitrogen sweep with constant flow. The reaction was carried out at 150 ºC, for about 9 h and the final product was properly stored.

The functionalization of the OligLA was performed with IEMA, an isocyanate-functional monomer containing carbon double bonds. The amount of IEMA added was set to fulfill total conversion of the isocyanate groups. Diethyl ether (20 mL per 0.02 mol of oligomer) was previously added to OligLA to promote the dissolution of IEMA (0.04 mol) in the previous mixture. The reaction was allowed to proceed in a three-neck round-bottom flask at 60 °C, under reflux and magnetic stirring, for 24 h. The functionalized oligomer will be further designated as macLA-IEMA.

2.2.3. Preparation of the copolymers and respective photocrosslinking

The preparation of the copolymers was carried out by homogeneously mixing UP with macLA-IEMA, varying the mass proportions in the blend. The obtained copolymers were designated as 1:1, 2:1 and 1:2 (depending on the ratio of UP:macLA-IEMA).
The amount of Ir2959 added to each prepared copolymer was 6% of the carbon double bonds moles. The final mixture was stirred under heat, until a homogeneous solution was obtained. Further, the product was poured onto glass plates and uniformly spread with the aid of a stainless-steel cylinder, in the order to obtain transparent and flexible films, with 1 mm of thickness, after 2 minutes and 30 seconds of UV irradiation. The UV lamp used was a Multiband UV UVGL-48 wavelength 254-354 nm from Mineral Light® Lamp, in the 254 nm wavelength setting. Once completed the UV irradiation, transparent, uniform and flexible films were achieved.

2.3. Characterization techniques

2.3.1. Nuclear Magnetic Resonance (NMR)

The ^{1}H NMR spectra of the UP, oligomers and macromers, were obtained on a 9.4 Tesla Spectrometer, using a 3 mm broadband NMR probe in deuterated tetrahydrofuran (THF-d8), at room-temperature. Tetramethylsilane (TMS) was used as the internal reference.

2.3.2. Rheological studies

A controlled stress rheometer, Haake, model RS1, was used to measure the viscosity. The geometry used was a plate/plate system PP20 (titanium for the rotating part and stainless steel for the stationary part). Rheological behavior of the prepared polyesters was assessed at 25 °C and viscosities as function of the shear rate over time were determined. All measurements were made in triplicate.

2.3.3. Dynamic contact angles

The dynamic contact angles of the films were measured in a Dataphysics OCA-20 contact angle analyzer (DataPhysics Instruments, Filderstadt, Germany) using the sessile drop method. A droplet of deionized water (10 μL) was automatically dispersed onto the sample surface and its evolution along time was recorded with a CCD video camera attached to the equipment. The water contact angles were automatically calculated by the equipment software. The data obtained represents the mean values of at least three independent measurements.

2.3.4. Gel content

In order to attain a qualitative analysis of the crosslinking process, the materials gel content was determined by solvent extraction. Samples of dried films, with the dimensions of 2x1x1 cm, were weighted (W_i) and immersed in diethyl ether overnight in sealed containers (under stirring, at room temperature). The samples were afterwards removed, dried, and reweighted (W_f). Gel content was determined as represented in Eq. 1.

$$\text{Gel content (\%)} = \left(\frac{W_f}{W_i}\right) \times 100 \quad (1)$$

2.3.5. Water sorption capacity

Four samples of each produced film, with the dimensions of 2x1x1 cm, were prepared and weighed (W_d). The dried samples were placed in a desiccator containing a saturated solution of pentahydrate copper sulfate, at a relative humidity of 95%, at room temperature. Specimens of each sample were removed and weighted at predetermined times (W_s) until maximum weight was achieved.

Finally, the swelling capacity was assessed by using Eq. 2.

$$\text{Swelling (\%)} = \left(\frac{W_s - W_d}{W_d}\right) \times 100 \quad (2)$$

2.3.6. Hydrolytic degradation

For hydrolytic degradation, samples of the developed films (n=4), with the dimensions of 2x1cm, were previously dried in an vacuum oven at 50ºC and then weighted ($W_{d,o}$). Afterwards, they were immersed in PBS 0.01M (pH 7.4), and then incubated for six weeks at 37 ºC. At predetermined times (24h, 72h, 1, 2, 3, 4, 5 and 6 weeks), the films were removed from PBS, washed with distilled water and dried in vacuum conditions, at 37 ºC, until constant weight ($W_{d,t}$). The degree of degradation was calculated from the weight loss, which was determined as presented in the Eq. (3).

$$\text{Weight loss (\%)} = \frac{W_{d,0} - W_{d,t}}{W_{d,0}} \times 100 \quad (3)$$

where $W_{d,o}$ and $W_{d,t}$ are the samples average weights before the degradation test and at time *t*, respectively. An average of four measurements was performed.

The biodegradation profiles of the films (Fig.6) were determined through the incubation of the prepared adhesive (n=4), in PBS (pH 7.4), at 37 ºC, for a total of 6 weeks, to simulate physiological conditions.

2.3.7. Dynamic mechanical thermal analysis

The photocrosslinked samples were analyzed by Dynamical Mechanical Thermal Analysis using a Triton Tritec 2000 in the Single Cantilever Bending mode and in multifrequency conditions (1, 10 Hz) with a standard heating rate of 5 °C·min^{-1}. The glass transition temperature (T_g) was determined as the peak in tan δ (tan δ = E″/E′), where E″ and E ′ are the loss and storage modulus, respectively.

2.3.8. Characterization of the biological properties of the produced bioadhesives

2.3.8.1. Evaluation of the cell viability and proliferation in contact with bioadhesive films

NHDF cells were cultured in DMEM-F12, supplemented with 10% heat inactivated FBS, amphotericin B (100 g/mL) and gentamicin (100 g/mL) in 75 cm^2 culture T-flasks. Cells were maintained in a humidified atmosphere at 37°C, with 5% CO_2. Before cell seeding, bioadhesive films were placed into 96-well plates and sterilized by UV irradiation during 1h. After that, cells were seeded at a density of 10 x 10^3 cells per well to evaluate the cell adhesion and proliferation in the presence of the films.

The cytotoxic profile of the bioadhesives was characterized using an MTT assay that was performed according to the guidelines set by ISO 10993-5. Briefly, the medium was removed and 50 µL of MTT (5mg/mL PBS) were added to each sample (n=5), followed by their incubation for 4h, at 37°C, in a 5% CO_2 atmosphere. Then, cells were treated with 200 µL of DMSO (0.04N) for 30 min. A microplate reader (Biorad xMark microplate spectrophotometer) was used to read the absorbance at 570 nm of the samples from each well. Cells cultured without materials were used as negative control (K^-), whereas cells cultured with EtOH (96%) were used as positive control (K^+).

2.3.8.2. Characterization of cell adhesion to the surface of films through scanning electron microscopy

Cellular adhesion to the surface of the films was characterized by Scanning Electron Microscopy (SEM). The biological samples containing cells were washed with PBS and then fixed with 2.5 % (v/v) glutaraldehyde, overnight. Then, the samples were dehydrated with grading concentrations of EtOH solutions (50, 60, 70, 80, 90 and 99.9%) and freeze-dried for 3h. Finally, the samples were mounted onto aluminum stubs with Araldite glue and sputter-coated with gold using a Quorum Q150R ES sputter coater (Quorum Technologies Ltd, Laughton, East Sussex, UK). SEM images were then acquired with different magnifications, using an acceleration voltage of 20 kV, in a Hitachi S-3400N Scanning Electron Microscope (Hitachi, Tokyo, Japan) [28,29].

2.3.8.3. Evaluation of the antibacterial activity of the films

S. aureus (a Gram-positive bacterium that is the most common pathogen found in biomaterial associated infections) and *E. coli* (a Gram-negative bacterium commonly present in human organism) were used as model bacteria to evaluate the antimicrobial properties of the UP:macLA-IEMA films [30]. For this purpose, a modified Kirby-Bauer technique was used to characterize the antimicrobial properties of the bioadhesives. Briefly, the bacteria at a concentration of 1 x 10^8 CFU/mL were dispensed onto an agar plate. Then, circular bioadhesive films (n=3) were placed on the agar plate and incubated during 24h, at 37ºC [31]. After that, the inhibitory halo diameter induced by the films were photographed and measured using ImageJ (Scion Corp., Frederick, MD), image analysis software. Subsequently, SEM images were acquired to evaluate the biofilm formation at the surface of the material [32].

3. Results and Discussion

3.1. Synthesis

Different base prepolymers were synthesized and posteriorly functionalized and photocrosslinked. The components of the UP formulation were chosen based on the

biocharacter of the fumaric acid, since it's a naturally compound found in the organism (a component of the citric acid cycle), being expected that the non-reacted terminal groups would be biocompatible [33,34]. Moreover, PEG 600 was selected due to its hydrophilic character, which will counterbalance the hydrophobicity of the lactic acid oligomer, and hence improve hydrolytic degradation and cell interaction) [35]. Further, biodegradable polymers using PEG 600 have previously been prepared, evidencing its excellent biocompatibility and biodegradability [14,36,37].

Regarding the preparation of macLA-IEMA, low molecular weight oligomers (oligLA) with OH terminal groups were synthesized by direct dehydration of a L(+)-lactic acid solution using 1,4-butanediol as a reactive co-monomer. OligLA was then modified with the introduction of photocurable carbon-carbon double bonds and functionalized with IEMA. Furthermore, UP and macLA-IEMA were mixed together, creating three copolymers with different proportions of each materials (1:1, 2:1 and 1:2). The prepared copolymers were finally UV cured using Ir2959, yielding flexible crosslinked networks after 2 minutes and 30 seconds of irradiation. The synthesis processes are summarized in Fig.1.

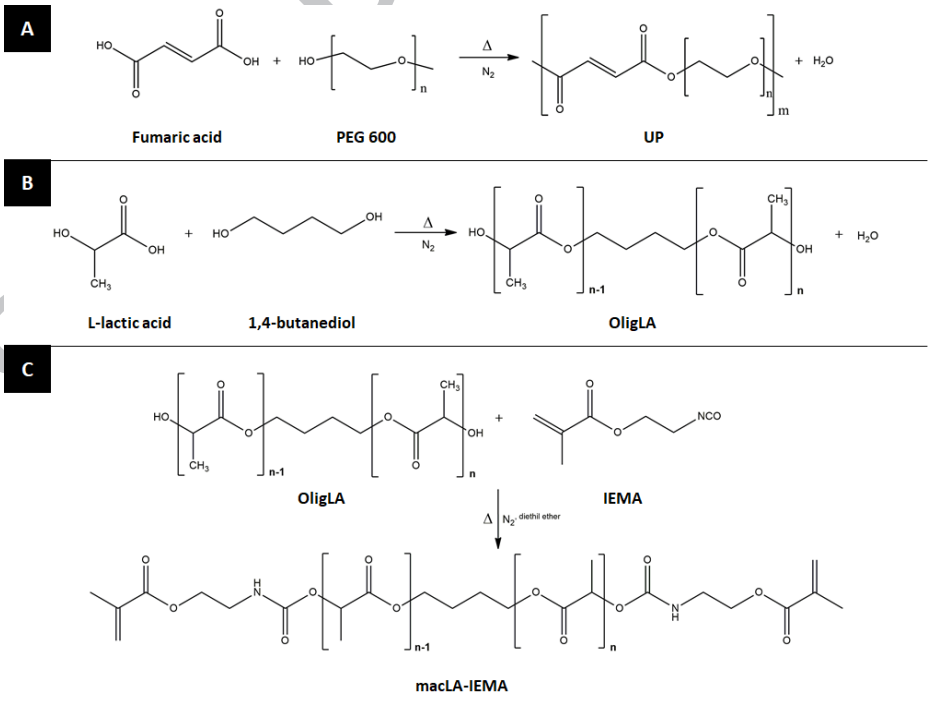

Figure 1. Schematic representation of the UP synthesis (A). Synthesis of OligLA based on L-lactic acid and 1,4-butanediol (B). Preparation of the macLA-IEMA by functionalization of the OligLA with IEMA (C).

3.2. NMR analysis

^{1}H NMR spectra of the synthesized UP and functionalized macromer macLA-IEMA are presented in Fig.2 and Fig.3, respectively. As can be seen by the ^{1}H NMR spectra in Fig.2, the UP synthesis was successful, with the signals at 6.86 and 6.79 ppm, assigned to the double bonds. The peak around 4.32 ppm was attributed to the ester bond -*COO-CH$_2$*- [38] while the signal at 3.73 ppm was due to -*CH$_2$-O*- protons in the molecular structure of the PEG 600 [24]. The peaks at 3.61 ppm and 3.50 ppm were assigned to the terminal CH_2 protons. The broad peak at 2.63 ppm was assigned to the terminal OH groups [21].

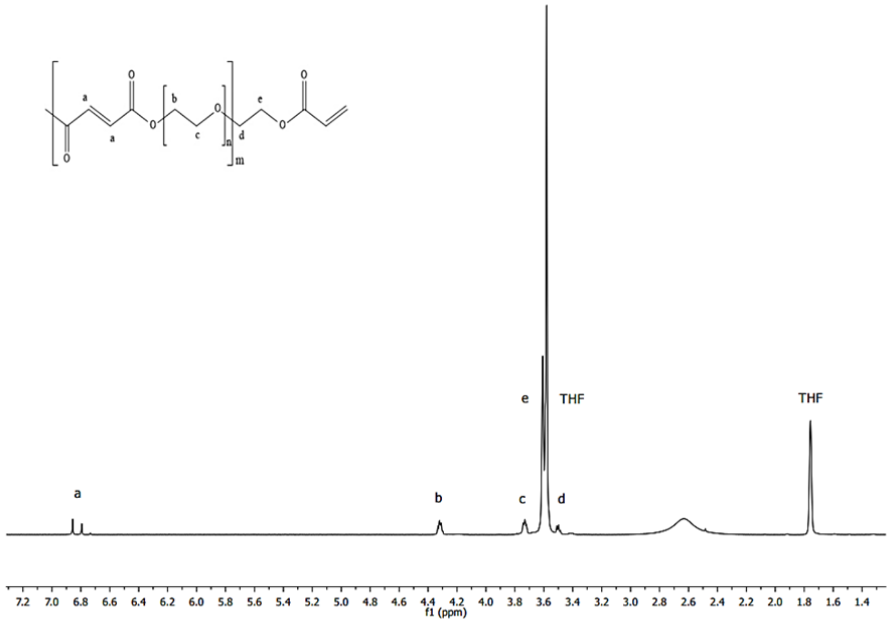

Figure 2. ^{1}H NMR spectra of UP. The numbered signals correspond to the protons assigned to the displayed structure [(a) δ = 6.86-6.79 (-*H*C=C*H*-), (b) δ = 4.32 (-COO-C*H$_2$*-), (c) δ = 3.73 (-C*H$_2$*-O- from PEG 600), (d) δ = 3.50 and (e) 3.61 (terminal CH_2)].

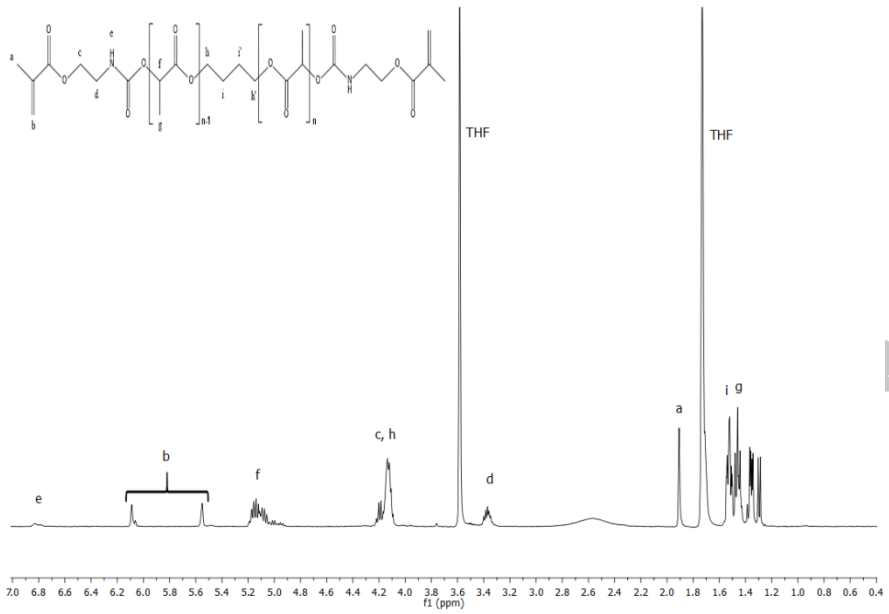

Figure 3. ^{1}H NMR spectra of macLA-IEMA. The numbered signals correspond to the protons assigned to the displayed structure [(a) δ = 1.90 (-C*H*$_3$ from methacrylate end functionalities), (b) δ = 5.5 and 6.00 (CH$_3$-C(C*H*$_2$)-COO- olefinic protons), (c) (h) δ = 4.23-4.10 (-O-C*H*$_2$-), (d) δ = 3.38 (-NH-C*H*$_2$-), (e) 6.83 (-CH$_2$-*NH*-C=O), (f) δ = 5.0-5.2 (-O-C*H*-(CH$_3$)-C=O), (g) δ = 1.5 (-O-CH-(C*H*$_3$)-C=O)].

According to the ^{1}H NMR spectrum of macLA-IEMA, there are two resonances at 6.00 ppm and 5.55 ppm, assigned to the olefinic protons [21,24,39]. The *CH*$_3$ methyl of the methacrylate end functionalities were assigned at 1.90 ppm while the signals at 3.38 ppm and 6.84 ppm were attributed to the -*NH*-*CH*$_2$- and to -*NH*-*C*=*O* protons, respectively. The signal at 6.83 ppm was ascribed to the -*CH*$_2$-*NH*-*C*=*O* protons. An overlap of peaks was observed from 4.23 to 4.10 ppm and were assigned to the -*O*-*CH*$_2$- protons.

3.3. Rheological studies

Rheological analysis was carried out in order to measure the viscosity as a function of increasing shear rate (Fig.4).

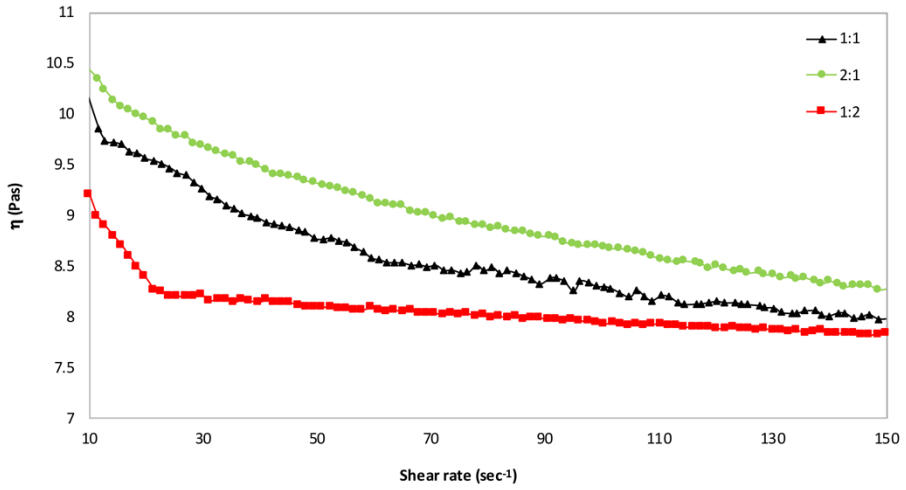

Figure 4. Rheological behavior of the polymeric blends.

From the obtained results, it can be observed that the initial values of viscosity are similar amongst the polymeric blends. However, the variation of viscosity when increasing shear rate differs between the samples. Shear viscosity of the polymeric blend with higher amount of macLA-IEMA presents two distinct regions: a shear thinning region at the low shear region followed by a Newtonian region. However, this Newtonian region disappears when the amount of UP is increased in the blend. Those samples present a shear thinning behaviour, characterized by decreasing viscosity with increasing shear rates [40], all through the experiment. The disappearance of the Newtonian region is due to the fact that UP is obtained by bulk polycondensation while macLA-IEMA is synthesised in diethyl ether. The presence of the solvents allows the disentanglement and alignment of the polymeric chains in the direction of the flow [41].

3.4. Dynamic contact angles

One of the most important surface properties that affects materials biological performance is its wettability, since the surface of the material is in direct contact with biological cells and fluids. The wettability of the materials surface plays a crucial role in biological events, such as protein adsorption, platelet adhesion, blood coagulation, as well as cell adhesion and proliferation [42,43]. This characteristic of the biomaterials can be evaluated by measuring the contact angles (CA) between a drop and the surface

of the material. The results obtained through the analysis of the dynamic contact angles of the produced adhesives are presented in Fig.5.

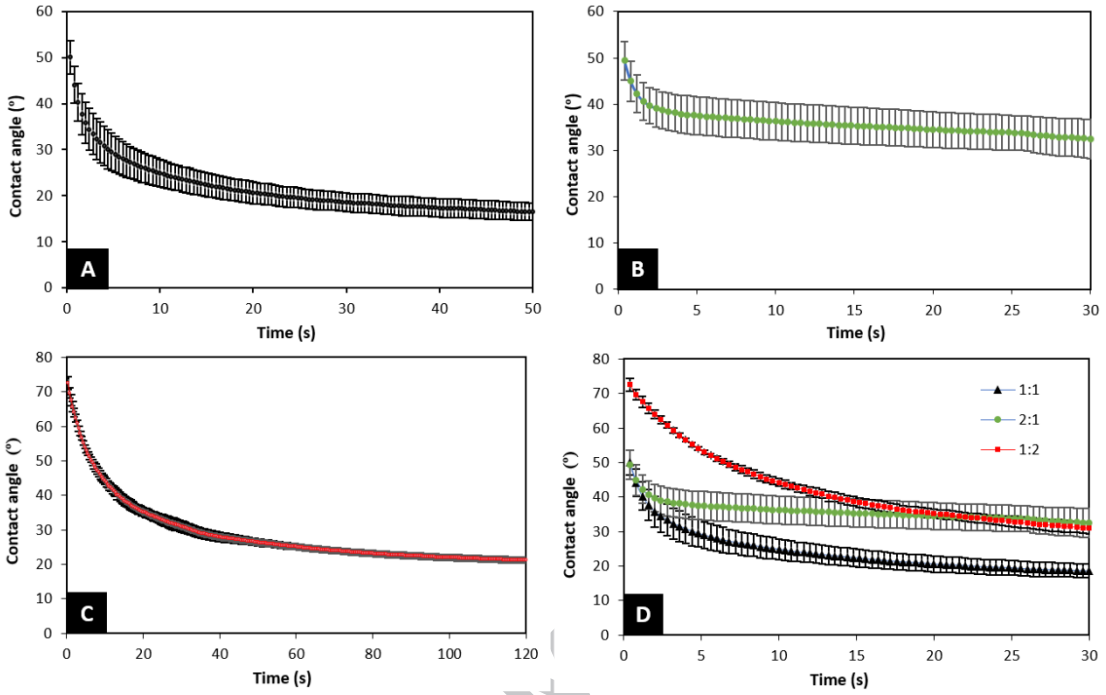

Figure 5. Dynamic water contact angles for 1:1 adhesive (A), 2:1 adhesive (B), 1:2 adhesive (C) and, comparison between the CA of the three adhesive formulations (D).

According to Fig.5, it is possible to verify that the three produced adhesives had low CA values, confirming their hydrophilic character. Such behavior was expected due to the incorporation of the naturally hydrophilic polymer (PEG) into the formulations, that at the surface of the wound dressings will ameliorate the cell adhesion, spreading and growth [32]. The 1:1 adhesive (Fig.5A) presented an initial contact angle value of ≈ 50°, and decreased to ≈ 16° in 50 seconds while 2:1 bioadhesive (Fig.5B) CA values decreased from 49º to 30° after 30 seconds. Also, during this analysis two distinctive behaviors were observed. The 1:1 and 2:1 adhesives showed a clear spreading of the drop in the material along 50 and 30 seconds, respectively. After this time, the drop is completely absorbed by the adhesive. By the contrary, the 1:2 adhesive (Fig.5C) presented the higher starting angle and a lower final CA of about 20° after 120 seconds of the test. In this case, the drop was not absorbed by the polymer matrix even after 120 seconds, and only a spreading over the surface of the material was observed. This result

was already expected, since the main goal of the incorporation of the macLA-IEMA was to enhance the hydrophobicity of the adhesives.

3.5. Gel content

The adhesives gel content was evaluated in order to determine the crosslinking degree, assuming that the films with 100% of gel content the total conversion of double carbon bonds. Among different factors, the crosslinking process proved to be dependent on the UV irradiation time, as can be observed in Tab.1.

Table 1. Curing times and respective gel content for the different adhesives formulations.

Adhesive	Curing time (min)	% gel content
1:1	2.5	74.2
	5	76.5
	10	78.8
	15	84.8
2:1	2.5	73.7
	5	75.7
	10	80.6
	15	81.0
1:2	2.5	86.1
	5	87.4
	10	87.7
	15	90.5

According to Tab.1, an increase on the UV irradiation time results in an increase of the gel content, and therefore the films become stiffer and more compact.

Furthermore, it was found that the 1:2 adhesive, mainly composed of macLA-IEMA, presented the highest percentage of gel content and, therefore, a higher degree of crosslinking. This result can be explained due to the higher amount of double bonds that macLA-IEMA assigns to the copolymer (higher than the UP).

3.6. Water sorption capacity

Immediately, after the occurrence of a wound, the healing process is initiated aiming to re-establish the structure and functions of the damaged tissue as soon as possible. To improve this process, the use of biological adhesives is an attractive approach to provide a constant mechanical support, promoting the cell interaction and proliferation [1]. Further, it is crucial that the excess of exudates produced at wound site are removed, since its presence promotes skin infections and tissue maceration [43,44]. To accomplish that, wound dressings must be able to absorb the excess of the wound exudates, providing a suitable moist microenvironment at the wound site [37].

Herein, water sorption capacity was determined for four samples of each synthesized adhesives, equally in a saturated controlled atmosphere of pentahydrate copper sulfate, at a relative humidity of 95%, for a total of 6 weeks. The results showed that swelling was more pronounced during the first 24 hours of saturation. However, from that period, the samples began to present a lower capacity of swelling, translated into a hydrated weight inferior to the initial dry weight. The release of a residual liquid by these materials was also observed. This event suggests that from the first 24 hours the adhesives began to undergo degradation by hydrolysis.

In Fig.6 the swelling results of bioadhesives are presented, where the 2:1 adhesive exhibits the highest swelling (22.2%), highlighting its hydrophilic character. This behavior can be explained by the high amount of PEG, characterized by hydrophilic long chains, capable of absorb high quantity of water, and therefore allowing the material to exert some pressure on the wound, leading to an improvement in hemostasis [24].

Contrarily, the 1:2 film presented the lower swelling profile (13.8%), corroborating their less hydrophilic character (CA $\approx$ 30°). Such fact can be explained by the incorporation of urethane bonds by the IEMA into the prepolymer terminations, which will interact with the hydrogen bonds, resulting in lower swelling.

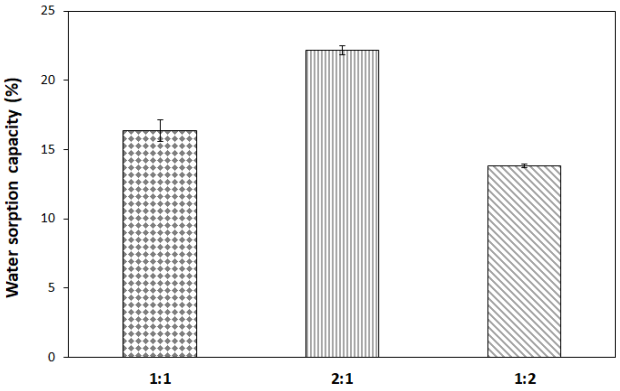

Figure 6. Swelling behavior of the synthesized adhesives after 6 weeks.

3.7. Hydrolytic degradation

The degradation of the bioadhesives can occur either by hydrolysis or by enzymatic action, for a sufficiently amount of time, allowing the complete healing of the incision. In addition, the products of degradation must be naturally metabolized by the body.

The biodegradation profiles of the films (Fig.6) were determined through the incubation of the prepared adhesive (n=4), in PBS (pH 7.4), at 37 ºC, for a total of 6 weeks, to simulate physiological conditions [45].

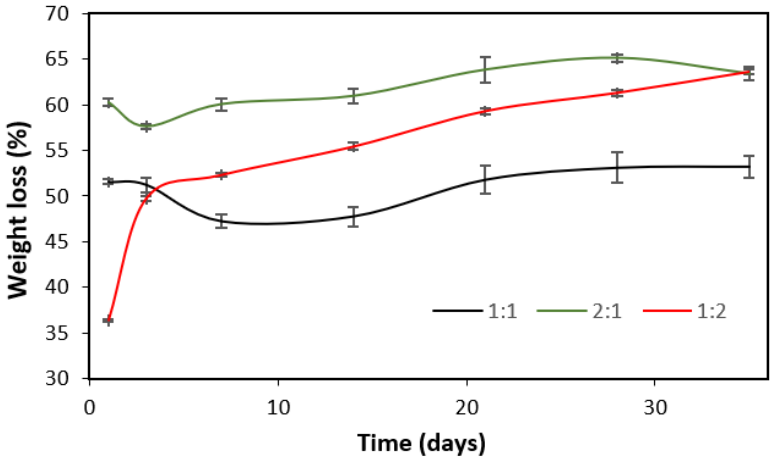

Figure 7. Hydrolitic degradation profile of the prepared bioadhesives.

After the first 24h, all bioadhesives presented a high weight loss %, which means that the unreacted molecules after UV irradiation and any residual solvent (diethyl ether) remaining within the matrix may be the cause of this abrupt weight loss in the first 24h

of incubation. Moreover, it was observed that the weight loss dependent on the degree of crosslinking, i.e., higher degree of crosslinking promoted a lower weight loss.

The 2:1 adhesive presented the higher initial weight loss percentage of 60 ± 0.42%, after 24 hours, since this formulation had a lower degree of crosslinking (as can see in Tab.1). After 3 days, the weight loss percentage stabilized to values of 65 ± 0.37%.

Regarding to the 1:2 adhesive (higher degree of crosslinking), it displayed an initial weight loss of 36 ± 0.14%, reaching the maximum value of 64 ± 0.24% after 6 weeks. In turn, the adhesive with a 1:1 molar ratio presented the lowest weight loss (around 51 ± 0.8%).

The biodegradation of these adhesive films results essentially from the hydrolysis of the ester bond present in the copolymers [17,46–48]. In this way, these results are well correlated with the water absorption capacity [49], *i.e*, the 2:1 adhesive presented the higher water uptake ability and also the higher weigh loss percentage. The improved ability to interact with water molecules will promote the expansion of the polymeric matrix, contributing for the acceleration of their hydrolytic degradation. On the contrary, the behavior of the 1:2 adhesive in the first 24 hours can be explained, since this formulation contained a larger amount of the macromer, which may have been responsible for a greater degree of crosslinking of this adhesive, and consequent increase of stiffness.

Furthermore, it is worth to notice that this biodegradation profile can suffer severe changes in *in vivo* conditions, since the presence of the enzymes, pH, and cell components will affect the degradation process [50].

3.8. Thermal properties

DMTA technique was used to identify the glass transition temperature (T_g) of the adhesives. Fig.8 shows that the T_g is lower than physiological temperature in all adhesive formulations, between -36 °C and -20 °C, therefore fulfilling an important requirement for the intended purpose, and no crystallization was observed. It was also noticed that all thermograms, only one frequency-sensitive peak was visible, indicating that the components are perfectly miscible. Thus, all materials have negative T_g values,

which means that they are flexible materials at room temperature, as well as at physiological temperature. In addition, it is found that increasing the OligLA ratio in the copolymer composition induced an increase in its T_g, revealing that its incorporation decreases the freedom of movement of the polymer chains.

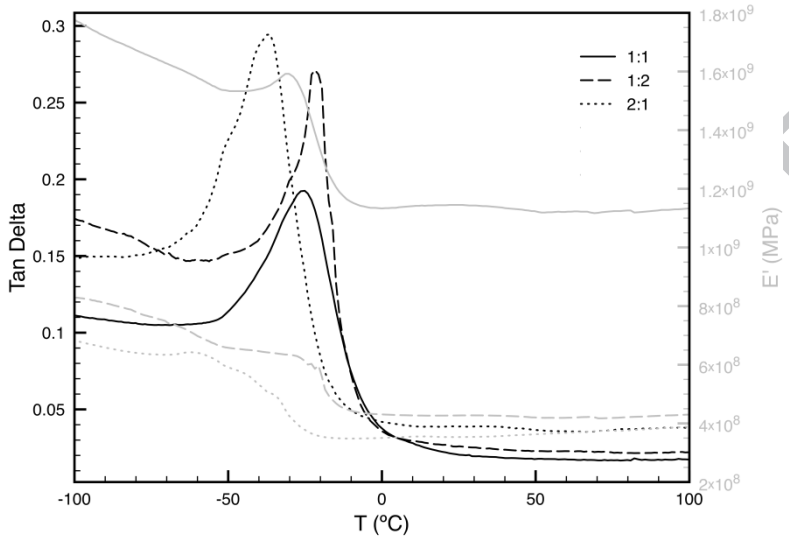

Figure 8. DMTA analysis of bioadhesives.

3.9. Biological properties of the films

3.9.1. Characterization of the cell viability and adhesion in contact with bioadhesive films

To evaluate the cytotoxic character of the bioadhesive films, NHDF were used as model cells. NHDF were selected since they interact with the surrounding cells and they are involved in production of the extracellular matrix and molecules essential for wound healing process to occur [51,52].

Optical microscopic images of the NHDF cells in contact with films after 1, 3 and 7 days are presented in Fig.9. These images indicate that NHDF cells did not suffer any morphological variation when seeded in contact with films, exhibiting a similar morphology to those of K^-, where cells were incubated with culture medium.

In addition, the cell viability was also characterized though an MTT assay during 1, 3 and 7 days. The metabolic conversion of MTT, a yellow tetrazole salt, to purple formazan crystals occurs in living cells, indicating the number of the viable cells present in each well [53]. The data obtained from the MTT assay (Fig.9A) revealed that the 1:1

and 2:1 adhesives did not affect the cell viability for 7 days. Nonetheless, the 1:2 film presented a decrease in cell viability after 3 and 7 days of incubation.

On the other side, the interaction between cells and bioadhesives films were evaluated by SEM. Fig.10B evidenced the excellent adhesive properties of the 1:1 and 2:1 adhesives. In these formulations, the cells presented various filopodia protrusions, indicating that NHDF cells adhered, spread and proliferated at films' surface.

Considering all the data gathered *in vitro*, the 1:1 and 2:1 adhesives exhibited the better biological performance to be used as surgical adhesive, since these formulations did not compromise the cell viability, promoting their attachment, spread and proliferation.

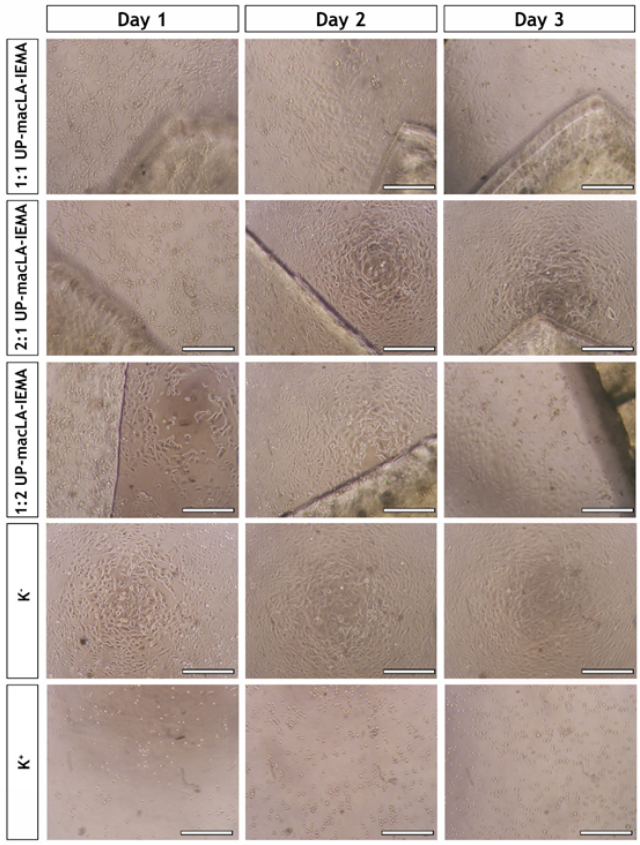

Figure 9. Optical microscopic images of Normal Human Dermal Fibroblast (NHDF) cells cultured in the presence of the different produced films after 1, 3, and 7 days of incubation; K^- (negative control); K^+ (positive control). Scale bar represents 200 µm.

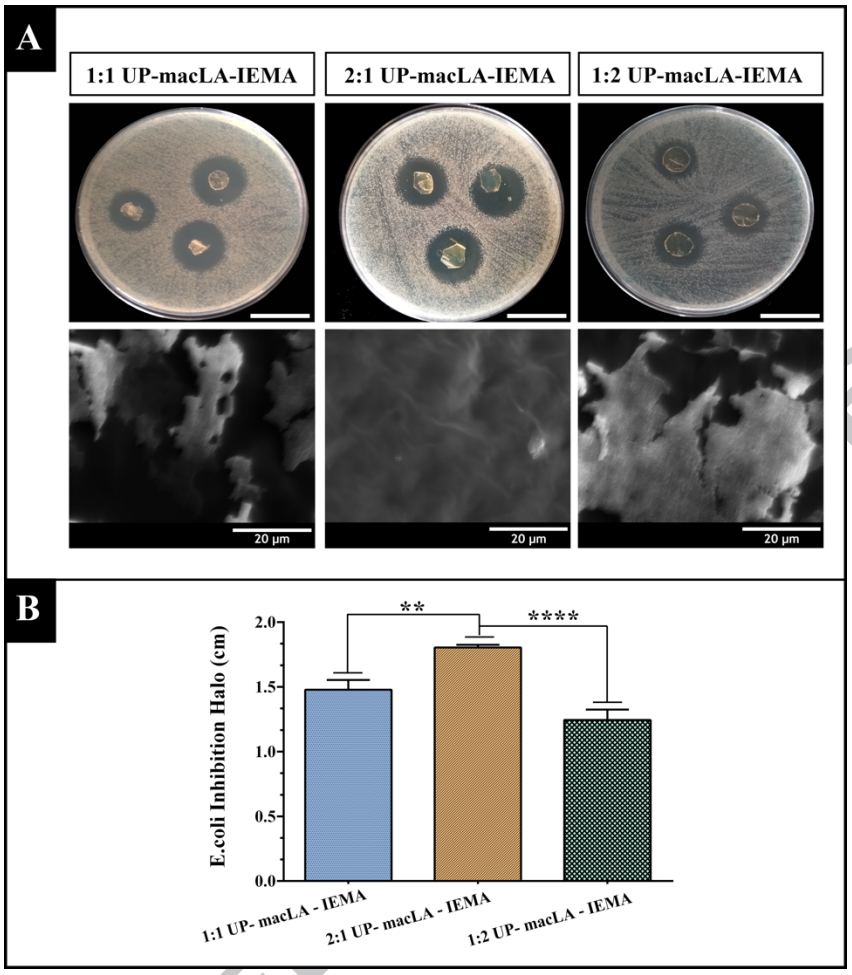

Figure 10. Characterization of the cytotoxic profile of the films through the analysis of the NHDF viability after 1, 3 and 7 days of incubation with films (A). K^- (negative control); K^+ (positive control). Data are presented as the mean ± standard deviation, n = 5, *p<0.05; SEM images of the NHDF morphology seeded at the surface of the different films after 1, 3 and 7 days (B).

3.9.2. Antibacterial activity

The bacterial contaminations are currently identified as the most severe and devastating complications associated with the implantation of biomaterials into the human body. Currently, it is estimated that 65-80% of bacterial infections are originated through the organisms that form biofilms on biomaterials' surface, compromising their successful implantation [44,54,55]. In this context, the production of antimicrobial biomaterials is crucial to avoid the infections related to their implantation growth. In this study, the antimicrobial properties of the produced bioadhesives were characterized by using *S.*

aureus (gram-positive bacterium) and *E. coli* (gram-negative bacterium). Herein, the inhibitory area was determined, and the biofilm formation was characterized by SEM analysis.

The results showed in Fig.11 demonstrated that 2:1, 1:1 and 1:2 formulations displayed inhibition halo with a diameter of 1.80 ± 0.02 cm, 1.48 ± 0.07 cm and 1.24 ± 0.08 cm against *E.coli*, respectively. In turn, the 2:1, 1:1 and 1:2 formulations presented inhibition halo' diameter of 1.85 ± 0.04 cm, 1.20 ± 0.07 cm and 0.1 ± 0.02 cm against *S.aureus*, respectively (as showed in Fig. 12). Taking into account the obtained results, it can be noticed that all the produced adhesives presented an antibacterial effect against *E.coli* and *S.aureus*. However, the antibacterial effect was more pronounced in 2:1 adhesive in comparison with 1:1 and 1:2 formulations. Such improved ability to avoid the bacterial growth was also noticed in the biofilm analysis, where no adhered bacteria was visualized. Such result can be explained by the higher amount of UP into 2:1 formulation, that has been already described in the literature as antifouling polymer. This antifouling surface possess bacteriostatic activity, delaying the biofilm formation and consequently will prevent the bacterial growth [56]. The PEG-based surfaces have been identified as antifouling surfaces, which can resist to the protein adsorption and subsequently prevent the bacterial adhesion [57–60]. Furthermore, these results are in accordance with other antifouling surfaces reported in the literature. For example, Wang and their collaborators developed an antifouling coating composed of HTCC-b-pSBMA, which avoid the colonization of *E.coli*, *Pseudomonas aeruginosa* and *Proteus mirabilis* microorganisms [61]. On the other side, Li *et al*. immobilized silver nanoparticles at poly(vinylidene fluoride) membranes, exhibiting excellent antifouling activity against *E.coli* and *S.aureus* [62].

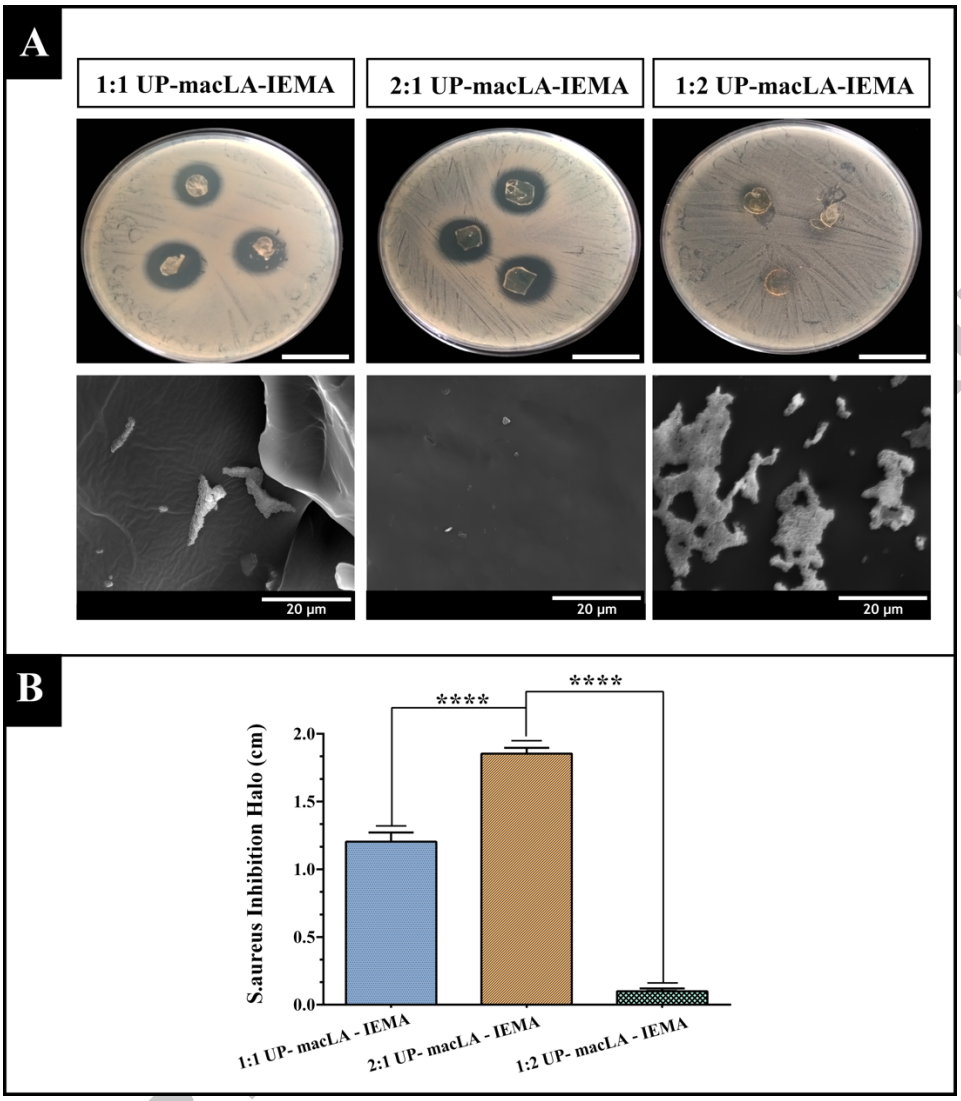

Figure 11. Evaluation of the antimicrobial properties of the adhesive films against *E.coli*: macroscopic visualization of the inhibition halos (A) and determination of the inhibition halos diameter displayed by the films (B). Data are presented as the mean ± standard deviation, n = 5, **p < 0.01, ****p < 0.0001.

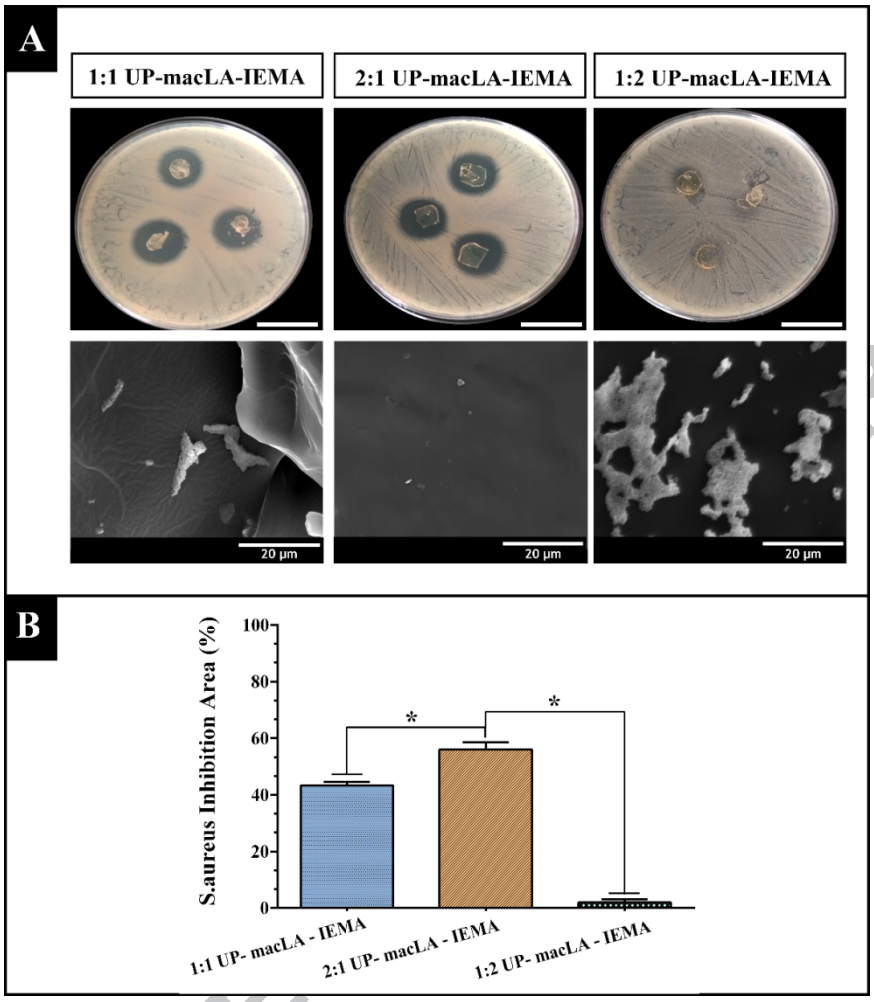

Figure 12. Evaluation of the antimicrobial properties of the adhesive films against *S.aureus*: macroscopic visualization of the inhibition halos (A) and determination of the inhibition halos diameter displayed by the films (B). Data are presented as the mean ± standard deviation, n = 5, ****p < 0.0001.

4. Conclusions

This paper reports the successful synthesis of new surgical adhesives, based on UP and lactic acid oligomers functionalized with IEMA. The obtained photocrosslinkable biodegradable copolymers, after 2 minutes and 30 seconds of UV irradiation, showed to be resistant, flexible and with suitable viscosity for the attended application. Moreover, despite further studies are required to quantify energy release during polymerization reactions, preliminary tests undertaken over bovine muscle tissue showed no signs of damage on that organic substrate meaning that heat release will not be a constraint.

It was shown that the developed adhesives presented a strong hydrophilic character and high gel contents. Overall, the three adhesives presented similar properties however, the different ratio in their formulations translated in distinct behaviors. It was found that the increase of PEG amount in the 2:1 formulation resulted in a higher water absorption capacity and consequently suffered in the first 24 hours a great weight loss. DMTA analysis showed glass transition temperatures in the range of -30 ºC to -20 ºC, confirming the flexibility and miscibility of the components in the adhesives. Initial studies concerning the stability of these materials overtime have shown that blends are stable even with solubilized Irgacure® 2959 for periods of over one year, as long as they are preserved from light sources.

The *in vitro* studies showed that the 1:1 and 2:1 bioadhesive films revealed a biocompatible character during 7 days in contact with human fibroblasts, since cell viability was not affected in contact with the samples. Further these materials prompted the cell adhesion and proliferation at their surfaces. Considering the obtained results, the biodegradable photocrosslinkable bioadhesives produced, in particular the 1:1 and 2:1 formulation exhibited the most auspicious properties to be applied as surgical bioadhesive.

Acknowledgments

This work was supported by the Portuguese Foundation for Science and Technology (FCT) (IF/01432/2015). The financial support of 73100, Lda and from POCI-01-0145-FEDER-03146 is also gratefully acknowledged. The team from CICS-UBI would like to acknowledge the financial support from FEDER funds through the POCI—COMPETE 2020—Operational Programme Competitiveness and Internationalization in Axis I—Strengthening research, technological development and innovation (Project POCI-01-0145-FEDER- 007491) and National Funds by FCT—Foundation for Science and Technology (Project UID/Multi/00709/2013). Sónia P. Miguel acknowledges a PhD fellowship from FCT (SFRH/BD/109563/2015).

DATA AVAILABILITY

The raw/processed data required to reproduce these findings cannot be shared at this time due to technical or time limitations.

References

[1] A. P. Duarte, J. F. Coelho, J. C. Bordado, M. T. Cidade, and M. H. Gil, "Surgical adhesives: Systematic review of the main types and development forecast," *Prog. Polym. Sci.*, vol. 37, no. 8, pp. 1031–1050, 2012.

[2] P. Ferreira, J. F. J. Coelho, and M. H. Gil, "Development of a new photocrosslinkable biodegradable bioadhesive," *Int. J. Pharm.*, vol. 352, no. 1–2, pp. 172–181, 2008.

[3] P. Ferreira, J. F. J. Coelho, J. . F. Almeida, and M. H. Gil, *Photocrosslinkable Polymers for Biomedical Applications*, no. 3. IntechOpen, 2011.

[4] R. Bitton, E. Josef, I. Shimshelashvili, K. Shapira, and D. Seliktar, "Phloroglucinol-based biomimetic adhesives for medical applications," *Acta Biomater.*, vol. 5, no. 5, pp. 1582–1587, 2009.

[5] T. C. M. C. W. Committe, "A novel collagen-based composite offers effective hemostasis for multiple surgical indications : Results of a randomized controlled trial," *Surgery*, vol. 129, no. 4, pp. 445–450, 2001.

[6] R. Article and J. T. Haemost, "The role of collagen in thrombosis and hemostasis," pp. 561–573, 2004.

[7] N. Annabi, K. Yue, A. Tamayol, and A. Khademhosseini, "Elastic sealants for surgical applications," *Eur. J. Pharm. Biopharm.*, vol. 95, pp. 27–39, 2015.

[8] K. A. Bresnahan, J. M. Howell, and J. Wizorek, "Comparison of Tensile Strength of Cyanoacrylate Tissue Adhesive Closure of Lacerations Versus Suture Closure," *Ann. Emerg. Med.*, vol. 26, no. 5, pp. 575–578, 1995.

[9] L. Li and H. Zeng, "Marine mussel adhesion and bio-inspired wet adhesives," *Biotribology*, vol. 5, pp. 44–51, 2016.

[10] G. Ak, E. Alpkilic Baskirt, E. Kurklu, M. Koray, H. Tanyeri, and B. Zulfikar, "Evaluation of Fibrin Sealants and Tissue Adhesives in Oral Surgery for Patients with Bleeding Disorders," *Turkish J. Hematol.*, vol. 29, no. 1, pp. 40–47, 2012.

[11] L. F. M. Silva, A. Öchsner, and R. D. Adams, *Handbook of Adhesion Technology*. Springer-Verlag Berlin Heidelberg, 2011.

[12] R. S. Benson, "Use of radiation in biomaterials science," *Nucl. Instruments Methods Phys. Res. B*, vol. 191, no. 1–4, pp. 752–757, 2002.

[13] J. H. Moon, Y. G. Shul, S. Y. Hong, Y. S. Choi, and H. T. Kim, "A study on UV-

curable adhesives for optical pick-up: I. Photo-iniciator effects," *Int. J. Adhes. Adhes.*, vol. 25, no. 6, pp. 534–542, 2005.

[14] M. Mehdizadeh and J. Yang, "Design Strategies and Applications of Tissue Bioadhesives," *Macromol. Biosci.*, vol. 13, no. 3, pp. 271–288, 2013.

[15] J. L. Ifkovits and J. A. Burdick, "Review: Photopolymerizable and Degradable Biomaterials for Tissue Engineering Applications," *Tissue Eng.*, vol. 13, no. 10, pp. 2369–2385, 2007.

[16] A. S. Karikari, W. F. Edwards, J. B. Mecham, and T. E. Long, "Influence of peripheral hydrogen bonding on the mechanical properties of photo-cross-linked star-shaped poly(D,L-lactide) networks," *Biomacromolecules*, vol. 6, no. 5, pp. 2866–2874, 2005.

[17] I. Vroman and L. Tighzert, "Biodegradable polymers," *Materials (Basel).*, vol. 2, no. 2, pp. 307–344, 2009.

[18] A. J. R. Lasprilla, G. A. R. Martinez, B. H. Lunelli, A. L. Jardini, and R. M. Filho, "Poly-lactic acid synthesis for application in biomedical devices - A review," *Biotechnol. Adv.*, vol. 30, no. 1, pp. 321–328, 2012.

[19] C. Ha *et al.*, "Bioactive cell-derived matrices combined with polymer mesh scaffold for osteogenesis and bone healing," *Biomaterials*, vol. 50, pp. 75–86, 2015.

[20] N. Uzun *et al.*, "Poly(l-lactic acid) membranes: Absence of genotoxic hazard and potential for drug delivery," *Toxicol. Lett.*, vol. 232, no. 2, pp. 513–518, 2015.

[21] J. M. C. Santos *et al.*, "Synthesis, functionalization and characterization of UV-curable lactic acid based oligomers to be used as surgical adhesives," *React. Funct. Polym.*, vol. 94, pp. 43–54, 2015.

[22] D. R. S. Travassos *et al.*, "Engineering star-shaped lactic acid oligomers to develop novel functional adhesives," *J. Mater. Res.*, vol. 33, no. 10, pp. 1463–1474, 2018.

[23] D. S. Marques *et al.*, "Functionalization and photocuring of an L-lactic acid macromer for biomedical applications," *Int. J. Polym. Mater. Polym. Biomater.*, vol. 65, no. 10, pp. 497–507, 2016.

[24] D. S. Marques *et al.*, "Photocurable bioadhesive based on lactic acid," *Mater. Sci. Eng. C*, vol. 58, no. January, pp. 601–609, 2016.

[25] S. M. Ho and A. M. Young, "Synthesis, polymerisation and degradation of poly(lactide-co-propylene glycol) dimethacrylate adhesives," *Eur. Polym. J.*, vol.

42, no. 8, pp. 1775–1785, 2006.

[26] F. A. M. M. Gonçalves, A. C. Fonseca, M. Domingos, A. Gloria, A. C. Serra, and J. F. J. Coelho, "The Potential of Unsaturated Polyesters in Biomedicine and Tissue Engineering: Synthesis, Structure-Properties Relationships and Additive Manufacturing," *Prog. Polym. Sci.*, 2016.

[27] C. G. Williams, A. N. Malik, T. K. Kim, P. N. Manson, and J. H. Elisseeff, "Variable cytocompatibility of six cell lines with photoinitiators used for polymerizing hydrogels and cell encapsulation," *Biomaterials*, vol. 26, no. 11, pp. 1211–1218, 2005.

[28] P. Coutinho, S. P. Miguel, I. J. Correia, P. I. Morgado, and M. P. Ribeiro, "Dextran-based hydrogel containing chitosan microparticles loaded with growth factors to be used in wound healing," *Mater. Sci. Eng. C*, vol. 33, no. 5, pp. 2958–2966, 2013.

[29] P. H. Castilho *et al.*, "Modification of microfiltration membranes by hydrogel impregnation for pDNA purification," *J. Appl. Polym. Sci.*, vol. 132, no. 21, p. 41610, 2015.

[30] A. C. L. Batista, G. C. Dantas, J. Santos, and R. V. S. Amorim, "Antimicrobial Effects of Native Chitosan against Opportunistic Gram-negative Bacteria," *Microbiol. J.*, vol. 1, no. 3, pp. 105–112, 2011.

[31] K. Kim *et al.*, "Incorporation and controlled release of a hydrophilic antibiotic using poly(lactide-co-glycolide)-based electrospun nanofibrous scaffolds," *J. Control. Release*, vol. 98, no. 1, pp. 47–56, 2004.

[32] S. P. Miguel, M. P. Ribeiro, H. Brancal, P. Coutinho, and I. J. Correia, "Thermoresponsive chitosan-agarose hydrogel for skin regeneration," *Carbohydr. Polym.*, vol. 111, pp. 366–373, 2014.

[33] D. W. Grijpma, Q. Hou, and J. Feijen, "Preparation of biodegradable networks by photo-crosslinking lactide, caprolactone and trimethylene carbonate-based oligomers functionalized with fumaric acid monoethyl ester," *Biomaterials*, vol. 26, no. 16, pp. 2795–2802, 2005.

[34] H. Shin, J. S. Temenoff, and A. G. Mikos, "In vitro cytotoxicity of unsaturated oligo[poly(ethylene glycol)fumarate] macromers and their cross-linked hydrogels," *Biomacromolecules*, vol. 4, no. 3, pp. 552–560, 2003.

[35] A. T. Metters, K. S. Anseth, and C. N. Bowman, "Fundamental studies of a novel, biodegradable PEG-b-PLA hydrogel," *Polymer (Guildf).*, vol. 41, no. 11,

pp. 3993–4004, 2000.

[36] L. S. Nair and C. T. Laurencin, “Polymers as biomaterials for tissue engineering and controlled drug delivery,” *Adv. Biochem. Eng. Biotechnol.*, vol. 102, no. October 2005, pp. 47–90, 2006.

[37] P. J. M. Bouten *et al.*, “The chemistry of tissue adhesive materials,” *Prog. Polym. Sci.*, vol. 39, no. 7, pp. 1375–1405, 2014.

[38] T. C. Haw, A. Ahmad, and F. H. Anuar, “Synthesis and characterization of poly(D,L-lactide)-poly(ethylene glycol) multiblock poly(ether-ester-urethane)s,” *AIP Conf. Proc.*, vol. 1678, no. October, p. 050025, 2015.

[39] A. C. Fonseca, I. M. Lopes, J. F. J. Coelho, and A. C. Serra, “Synthesis of unsaturated polyesters based on renewable monomers: Structure/properties relationship and crosslinking with 2-hydroxyethyl methacrylate,” *React. Funct. Polym.*, vol. 97, pp. 1–11, 2015.

[40] B. Abu-Jdayil, S. A. Al-Omari, H. Taher, and L. Al-Nuaimi, “Rheological characterization of clay-polyester omposites,” *Procedia Eng.*, vol. 10, pp. 716–721, 2011.

[41] C. J. Chirayil, L. Mathew, P. A. Hassan, M. Mozetic, and S. Thomas, “Rheological behaviour of nanocellulose reinforced unsaturated polyester nanocomposites,” *Int. J. Biol. Macromol.*, vol. 69, pp. 274–281, 2014.

[42] S. M. Oliveira, N. M. Alves, and J. F. Mano, “Cell interactions with superhydrophilic and superhydrophobic surfaces,” *J. Adhes. Sci. Technol.*, vol. 28, no. 8–9, pp. 843–863, 2014.

[43] S. P. Miguel, M. P. Ribeiro, P. Coutinho, and I. J. Correia, “Electrospun polycaprolactone/Aloe Vera_chitosan nanofibrous asymmetric membranes aimed for wound healing applications,” *Polymers (Basel).*, vol. 9, no. 5, 2017.

[44] S. P. Miguel, D. Simões, A. F. Moreira, R. S. Sequeira, and I. J. Correia, “Production and characterization of electrospun silk fibroin based asymmetric membranes for wound dressing applications,” *Int. J. Biol. Macromol.*, vol. 121, pp. 524–535, 2019.

[45] C. Zhu, S. R. Kustra, and C. J. Bettinger, “Photocrosslinkable biodegradable elastomers based on cinnamate- functionalized polyesters,” *Acta Biomater.*, vol. 9, no. 7, pp. 7362–7370, 2013.

[46] M. E. Gomes and R. L. Reis, “Biodegradable polymers and composites in biomedical applications: from catgut to tissue engineering,” *Int. Mater. Rev.*, vol.

495, no. April, pp. 261–273, 2004.

[47] C. Engineer, J. Parikh, and A. Raval, "Review on Hydrolytic Degradation Behavior of Biodegradable Polymers," *Trends Biomater. Artif. Organs*, vol. 25, no. 2, pp. 79–85, 2011.

[48] C. S. Proikakis, N. J. Mamouzelos, P. A. Tarantili, and A. G. Andreopoulos, "Stability of DL -Poly (lactic acid) in Aqueous Solutions," *J. Appl. Polym. Sci.*, vol. 87, no. 5, pp. 795–804, 2003.

[49] S. Y. Lee, P. Valtchev, and F. Dehghani, "Synthesis and purification of poly(l-lactic acid) using a one step benign process," *Green Chem.*, vol. 14, no. 5, pp. 1357–1366, 2012.

[50] H. K. Makadia and S. J. Siegel, "Poly Lactic-co-Glycolic Acid (PLGA) as Biodegradable Controlled Drug Delivery Carrier," *Polymers (Basel).*, vol. 3, pp. 1377–1397, 2011.

[51] W. S. Kim *et al.*, "Wound healing effect of adipose-derived stem cells: A critical role of secretory factors on human dermal fibroblasts," *J. Dermatol. Sci.*, vol. 48, no. 1, pp. 15–24, 2007.

[52] D. R. Figueira, S. P. Miguel, K. D. de Sá, and I. J. Correia, "Production and characterization of polycaprolactone- hyaluronic acid/chitosan- zein electrospun bilayer nanofibrous membrane for tissue regeneration," *Int. J. Biol. Macromol.*, vol. 93, pp. 1100–1110, 2016.

[53] J. van Meerloo, G. J. Kaspers, and J. Cloos, "Cell Sensitivity Assays: The MTT Assay," in *Methods in Molecular Biology (Methods and Protocols), vol 731*, Humana Press, 2011, pp. 237–245.

[54] M. van Oosten *et al.*, "Real-time in vivo imaging of invasive- and biomaterial-associated bacterial infections using fluorescently labelled vancomycin," *Nat. Commun.*, vol. 4, no. 1, pp. 1–8, 2013.

[55] C. A. Fux, P. Stoodley, L. Hall-Stoodley, and J. W. Costerton, "Bacterial biofilms: A diagnostic and therapeutic challenge," *Expert Rev. Anti. Infect. Ther.*, vol. 1, no. 4, pp. 667–683, 2003.

[56] M. R. Nejadnik, H. C. van der Mei, W. Norde, and H. J. Busscher, "Bacterial adhesion and growth on a polymer brush-coating," *Biomaterials*, vol. 29, no. 30, pp. 4117–4121, 2008.

[57] I. Banerjee, R. C. Pangule, and R. S. Kane, "Antifouling coatings: Recent developments in the design of surfaces that prevent fouling by proteins, bacteria,

and marine organisms," *Adv. Mater.*, vol. 23, no. 6, pp. 690–718, 2011.

[58] T. Ekblad *et al.*, "Poly(ethylene glycol)-Containing Hydrogel Surfaces for Antifouling Applications in Marine and Freshwater Environments," *Biomacromolecules*, vol. 9, no. 10, pp. 2775–2783, 2008.

[59] S. Krishnan, C. J. Weinman, and C. K. Ober, "Advances in polymers for anti-biofouling surfaces," *J. Mater. Chem.*, vol. 18, no. 29, pp. 3405–3413, 2008.

[60] A. Arora and A. Mishra, "Antibacterial Polymers - A Mini Review," *Mater. Today Proc.*, vol. 5, no. 9, pp. 17156–17161, 2018.

[61] R. Wang, K. G. Neoh, and E. T. Kang, "Integration of antifouling and bactericidal moieties for optimizing the efficacy of antibacterial coatings," *J. Colloid Interface Sci.*, vol. 438, pp. 138–148, 2015.

[62] J.-H. Li, X.-S. Shao, Q. Zhou, M.-Z. Li, and Q.-Q. Zhang, "The double effects of silver nanoparticles on the PVDF membrane: Surface hydrophilicity and antifouling performance," *Appl. Surf. Sci.*, vol. 265, pp. 663–670, 2012.

Highlights

- Biodegradable bioadhesives were usefully obtained for surgical adhesives
- Photocrosslinkable biodegradable unsaturated polyesters-based copolymers synthesis
- The adhesives presented a strong hydrophilic character and high gel contents
- Cell viability was not affected during 7 days in contact with human fibroblast

Graphical abstract